北京师范大学-香港浸会大学联合国际学院

理工科技学部

Division of Science and Technology

Division of Science and Technology
Beijing Normal University – Hong Kong Baptist University
United International College
北京师范大学-香港浸会大学联合国际学院理工科技学部

Address: 2000 Jingtong Road, Tangjiawan, Zhuhai, Guangdong Province, the People's Republic of China. Postcode 519087
广东省珠海市唐家湾金同路2000号

Tel: +86(0)756-3620132
Email:uicdst@uic.edu.cn
https://dst.uic.edu.cn/
https://dst.uic.edu.cn/en/students/student_opportunities/science_and_technology_poster_presentation.htm

北京师范大学
香港浸会大学
联合国际学院
BEIJING NORMAL UNIVERSITY · HONG KONG BAPTIST UNIVERSITY
UNITED INTERNATIONAL COLLEGE

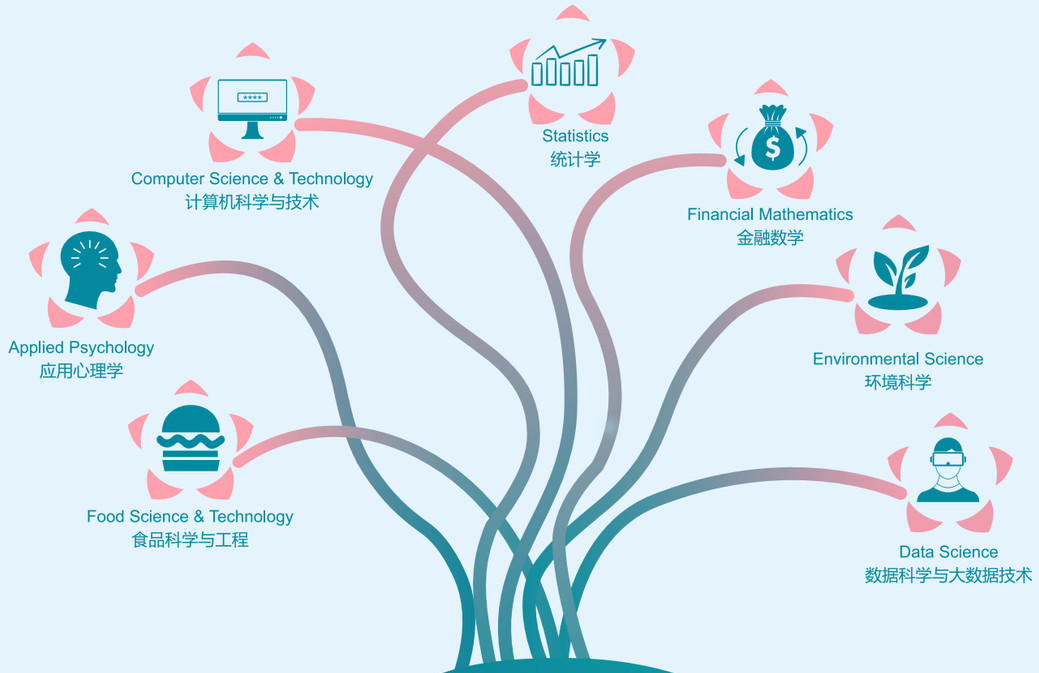

Selected Excellent Posters
of the 10th Science & Technology Poster Presentation

第十届理工科技学部优秀海报精选

13th April, 2022

校长寄语

正如美国总统富兰克林·罗斯福所说：“我们不能总是为我们的年轻人建设未来，但我们可以为未来建设我们的年轻人。”在UIC，我们一直致力于为我们的学生创造更多在实践中学习的机会，让他们更有能力建设祖国的未来。

我们理工科技学部（DST）的海报展，至2022年已经举办到第十届了。这是一个优秀的平台，不仅将科学和艺术等多类型学科结合在一起，给学生们提供了一个展示他们的努力与创造的平台，也凸显了我校一直以来推行的博雅教育的成果，我很高兴地看到参与每一届海报展的学生都展现出优秀的语言能力、艺术素养和丰富的想象力，他们已经从我们的校园汲取到充足的养分，准备好踏上更广阔的舞台。

在此，我祝贺DST再次成功举办了这届丰富多彩的海报展。也恭喜在此次海报展中的各位参加者和获奖者，你们的表现非常优秀，让我为我们的学校感到由衷的骄傲和自豪。

与此同时，我也想感谢DST的诸位教职员工和受邀的各行业专家，作为组织者、指导老师和评委，他们为这次活动慷慨地贡献了自己的时间和专业知识，学生们从中受益良多。他们也通过言传身教，给学生们竖立了好的榜样。

最后，我相信体验式学习才是最优质的学习。无论输赢，竞争的激情都能让我们的学生发挥出最好的一面。这些项目与海报让我们有机会一睹我们学生的未来及其可能性，这本身就是无价之宝。

汤涛

北京师范大学-香港浸会大学联合国际学院（UIC）校长

中国科学院院士

2022年4月22日

前言

十分感谢您阅读本届理工科技学部优秀海报精选。众所周知，让学生们从事研究活动是DST提供的独特教育体验的一部分。与往年一样，本届DST海报展所展出的海报均来自我们本科生的毕业设计（FYP）或研究生的研究项目。我很高兴所有参与的学生和他们的指导老师像往年一样，都提交了非常优秀的海报，并展现出极大的热情。

虽然由于突如其来的疫情，导致本次活动不得不采取线上线下同步进行的模式，我们依然进行了一些新颖的尝试，为本届海报展增添了不少亮色。在DST新成立的代间学院的支持下，我们成功邀请了很多中学生和部分学生家长参加本次活动，与我们各位海报展获奖者进行线上交流。我们的学生因此有了更多的机会通过他们的学术海报作品和演讲，与不同年龄段的人交流，这无疑令我们的学生受益，可以让他们学会从听众的角度思考问题，并加强他们发现问题和更清晰地提出解决方案的能力。这些能力是他们学习和未来事业的重要基础。

本次活动还首次刊印了这册优秀海报精选。一方面这本刊物可以让海报展的成果得以在学生与学生家长间得到更广泛的传播，展现我校学生的风采；另一方面它可以作为给海报展获奖者的一项特殊的奖励，为同学们留下一个美好的回忆，并鼓励以后的学生们更积极参与到这项活动中来。当然所有海报展的参与者们都已经获得了丰厚的回报：参与海报展过程中积累的丰富的研究经验，将为学生申请国内外知名学府的研究生提供极大帮助。

在此，我想借此机会感谢组委会举办这次活动。我还要特别感谢本次海报展的评委们，特别是受邀的校外评委，他们都是来自各个行业或其他高校的知名专家。他们不得不牺牲一整天的时间来为学生们提供有价值的意见和建议，相信学生从中获益良多。当然，最重要的是，我要感谢所有为制作这些海报努力学习并付出时间和经历的学生们，我在阅读这些海报时同样学到了很多。

潘建新教授

理工科技学部院长

2022年4月22日

Influencing Factors of Collective Efficacy in Small and Medium Enterprises: An Exploratory Study Using the Structural Equation Model (SEM) Approach

*D. S. Zhang**
Supervisor: Dr. G.W. Ho

中小企业员工集体效能感及其影响因素的结构方程模型研究

张迪申
指导老师：何义炜博士

Abstract: How to improve team performance is one of the top concerns of business managers, which has prompted scholars to study the factors influencing team performance. Previous studies have shown that collective efficacy is a strong predictor of team performance, which makes it a critical concept in business settings. Unfortunately, most previous research on efficacy beliefs has focused on the consequences of collective efficacy, while the antecedents of collective efficacy have not been well investigated. Therefore, this study aimed to explore the factors that influence the collective efficacy of corporate employees. Based on previous research, this study proposed a causal model of collective efficacy that included individual antecedents (self-efficacy, optimism) and organizational antecedents (leadership effectiveness, previous team performance, team cohesion). Self-report measures were used to gauge the variables in the proposed model, and structural equation modeling (SEM) was used to test the model. The results showed that organizational antecedents play a key role in predicting the collective efficacy of small and medium enterprise (SME) employees, while individual antecedents have a limited impact on the collective efficacy of SME employees. Based on the results, a four-factor causal model was developed. The model provides managers with a framework through which they can effectively improve employees' collective efficacy, thereby building a harmonious corporate environment and improving team performance.

摘要：集体效能感是指一个团体对其联合能力的共同信念，已被证明可以有效地预测团体的工作绩效。而如何提高团队绩效一直是企业管理者最关心的问题之一，因此，在商业环境下研究集体效能感具有很强的现实意义。然而，现有的文献大多聚焦于运动员群体，对于“什么会影响企业员工的集体效能感”这一关键问题缺乏研究。本研究着眼于这一研究空白，以中小企业员工为目标群体，在前人研究的基础上提出了关于集体效能感的因果模型，并采用结构方程模型（SEM）验证了该模型的有效性。该模型为想要提高员工集体效能感的中小企业管理者提供了一个指导性框架，揭示了培训中基层领导组织能力对于中小企业发展的重要性。

Influencing Factors of Collective Efficacy in Small and Medium Enterprises: An Exploratory Study Using the Structural Equation Model (SEM) Approach

D. S. Zhang*
Supervisor: Dr. G. W. Ho
Applied Psychology Programme, Division of Science and Technology, BNU-HKBU United International College
** Corresponding student author. Tel: +86-15670610899, E-mail: n830025135@mail.uic.edu.cn*

Abstract

How to improve team performance is one of the top concerns of business managers, which has prompted scholars to study the factors influencing team performance. Previous studies have shown that collective efficacy is a strong predictor of team performance, which makes it a critical concept in business settings. Unfortunately, most previous research on efficacy beliefs has focused on the consequences of collective efficacy, while the antecedents of collective efficacy have not been well investigated. Therefore, this study aimed to explore the factors that influence the collective efficacy of corporate employees. Based on previous research, this study proposed a causal model of collective efficacy that included individual antecedents (self-efficacy, optimism) and organizational antecedents (leadership effectiveness, previous team performance, team cohesion). Self-report measures were used to gauge the variables in the proposed model, and structural equation modeling (SEM) was used to test the model. The results showed that organizational antecedents play a key role in predicting the collective efficacy of SME employees, while individual antecedents have a limited impact on the collective efficacy of SME employees. Based on the results, a four-factor causal model was developed. The model provides managers with a framework through which they can effectively improve employees' collective efficacy, thereby building a harmonious corporate environment and improving team performance.

Introduction

Research Background

- **Key Variable:** Collective Efficacy
  - "A group's shared belief in its conjoint capabilities to organize and execute the courses of action required to produce given levels of attainments" (Bandura, 1997, p.477).
  - Collective efficacy has been proved to be a strong predictor of team performance.
- **Antecedents of Collective Efficacy:** Personal & Organizational

Personal Antecedents

- **Optimism**: "the extent to which people hold generalized favourable expectancies for their future" (Carver et al., 2010, p. 879)
- **Self-efficacy**: "the belief in one's ability to organize and execute the course of action required to produce given attainments" (Bandura, 1997, p. 3)

Organizational Antecedents

- **Leadership Effectiveness**: "group members' perceptions of the extent to which their group's leader provides task-related guidance and social-emotional support to subordinates" (Chen & Bliese, 2002, p. 549)
- **Previous Teamwork Performance**
- **Team Cohesion**: "the tendency of a team to unite in the pursuit of its goals regardless of difficulties and setbacks" (Verma et al., 2012, p. 45)

Research Question

Can these antecedents predict employees' collective efficacy well?

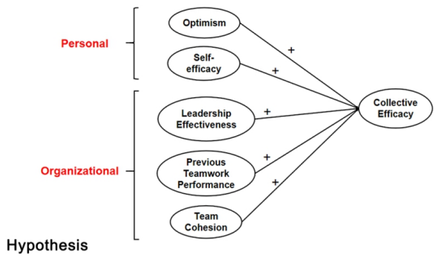

Hypothesis

There is no significant difference between the expected and sample covariance matrices.

Method

Participants

Ordinary staff from Henan You-de Medical Equipment Co., Ltd (Henan) and Print-Rite Co., Ltd (Zhuhai).
Total: 326 Valid: 272

Procedure

Informed Consent Form → Basic Personal Information → Scales

Data Analysis

- Descriptive Analysis (SPSS 21.0)
- Confirmatory Factor Analysis, Structural Equation Model (Amos 24.0)

Materials

Variable	Scale	Items	Author
Collective Efficacy	Work-related Collective Efficacy Scale	20	(Meng, 2001)
Self-efficacy	Work-related Self-efficacy Scale	17	(Meng, 2001)
Optimism	Optimism Personality Scale (OPS)	12	(Li, 2009)
Leadership Effectiveness	Leadership Effectiveness Scale	9	(Zhang, 2009)
Previous Teamwork Performance	Team Task Performance Measurement Scale	5	(Zhang, 2012)
Team Cohesion	Team Cohesion Scale	12	(Zhang, 2008)

Results

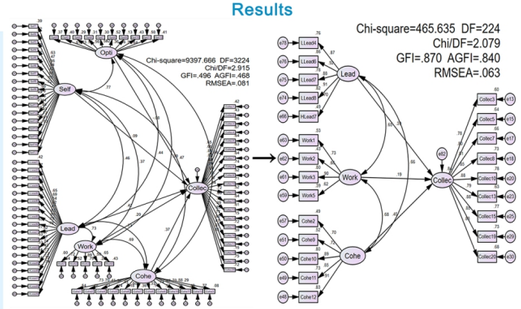

During the data analysis, it was evident that personal antecedents, including optimism and self-efficacy, had a weak and insignificant direct effect on collective efficacy in the structural equation model. Therefore, they were removed with the inappropriate items from the revised model.

Measurement Model

- **Convergent Validity** (Hair et al., 2010; Nunnally & Bernstein, 1994)
  - **Factor Loadings for all items were** > 0.6, ranging from 0.625 to 0.925 ($p < 0.001$)
  - **Composite Reliability (CR)** > 0.8, ranging from 0.821 to 0.952
  - **Average Extracted Variance (AVE)** > 0.5, ranging from 0.539 to 0.741
  - **Cronbach's α** > 0.8, ranging from 0.812 to 0.951
- **Discriminant Validity** (Hair et al., 2010)
  - The square root of AVE for all constructs > their correlation coefficients with other constructs

Structural Model

Model Fit Indexes	Model Value	Recommended Value	Overall Model Fit
Absolute Fit Indexes			
χ^2/df	2.079	>1.00, <3.00 (Schumacker & Lomax, 2004)	Yes
GFI	0.870	>0.80 (Doll et al., 1994)	Yes
AGFI	0.840	>0.80 (Doll et al., 1994)	Yes
SRMR	0.046	<0.05 (Wu, 2010)	Yes
RMSEA	0.063	<0.08 (McDonald & Ho, 2002)	Yes
Incremental Fit Indexes			
NFI	0.918	>0.90 (Wu, 2010)	Yes
CFI	0.956	>0.90 (Wu, 2010)	Yes
TLI	0.950	>0.90 (Wu, 2010)	Yes
IFI	0.956	>0.90 (Wu, 2010)	Yes
Parsimony Adjusted Indexes			
PNFI	0.813	>0.50 (Wu, 2010)	Yes
PGFI	0.706	>0.50 (Wu, 2010)	Yes

Model Stability: Cross-validation

$\Delta TLI < 0.05$; $|\Delta CFI| < 0.01$; $p \geq 0.05$ → the four-factor SEM has desired stability

Discussion

Contribution

- Establish an integrated model which offers theoretical support to study collective efficacy in business settings.
- Provide a framework for SMEs managers, through which they can effectively enhance the collective efficacy of their employees to improve the teamwork performance.

Implication: for SME managers

- The key to improving employees' collective efficacy lies in the organization.
- Enterprises should attach great importance to training lower-level leaders.

Limitation

Only recruited participants from entity enterprises, which reduced external validity of the results.

Conclusion

- Personal factors, including optimism and self-efficacy, have limited effect on employees' collective efficacy in small and medium enterprises.
- The analysis of the modified model (contains organizational antecedents only) supports the hypothesis.

References

1. Bandura, A. (1997). *Self-efficacy: The exercise of control*. W.H. Freeman.
2. Lent, R., Schmidt, J., & Schmidt, L. (2006). Collective efficacy beliefs in student work teams: Relation to self-efficacy, cohesion, and performance. *Journal of Vocational Behavior, 68*(1), 73-84. https://oi.org/10.1016/j.jvb.2005.04.001
3. Myers, N., Feltz, D., & Short, S. (2004). Collective Efficacy and *Team Performance: A Longitudinal Study of Collegiate Football Teams. Group Dynamics: Theory, Research, And Practice, 8*(2), 126-138. https://-doi.org/10.1037/1089-2699.8.2.126
4. Watson, C., Chemers, M., & Preiser, N. (2001). Collective Efficacy: A Multilevel Analysis. *Personality and Social Psychology Bulletin, 27*(8), 1057-1068. https://doi.org/10.1177/0146167201278012
5. Wu, M. L. (2010). *Structural equation model: manipulation in AMOS and application.* Chongqing University Press. (In Chinese)

The Design and Implementation of Multi-agent-based Quantum Trading System

B. H. Wu, C. H. Li
Supervisor: Dr. Raymond S. T. Lee

基于多智能体的量子交易系统的设计与实现

吴博卉、李川浩
指导老师：李树德博士

Abstract: Artificial Intelligence (AI) programs developed for traders to trade automatically received significant attention in both the financial industry and academia since trader programs in the financial market have grown rapidly in recent decades. However, many popular AI-based program trading models experienced the “black box effect,” where the model may produce excellent results for trading but fail to explain why the model would behave in a certain way. Genetic programming (GP), on the other hand, can generate and optimize human-interpretable rules and provide predictable model behavior, but many studies have shown that the rules cannot generate an excess return over the straightforward buy and hold strategy. In this project, we designed a multi-agent-based quantitative trading system that combines GP with quantum finance. A GP-based trading agent in the proposed system extracts trading rules from historical financial data and yields trading signals based on the rules learned. The quantum finance risk control agent manages the risk involved in the investment and optimizes using the genetic algorithm to adapt to different products dynamically. Statistical results show the system can generate excess returns over the buy-and-hold trading strategy at the Dow Jones Index from 2020 to 2021.

摘要：由于近几十年来金融市场上的自动化交易程序发展迅速，基于人工智能（artificial intelligence）的自动交易程序受到了金融业和学术界的广泛关注。然而，许多基于人工智能的自动交易模型存在“黑箱”效应——尽管模型可以提供出色的买入、持有、卖出信号，但未能解释模型的具体决策逻辑，从而引发投资者的质疑。相比之下，通过遗传编程（genetic programming）训练得到的模型具有可解释性，能带来稳定、可预测的模型行为。但许多研究表明，这些规则不能产生比买入并持有策略（buy and hold strategy）带来超额收益（excess return）。在此研究中，我们设计了一套基于多智能体（multi-agent）的量化交易系统，将遗传编程与量子金融结合起来。在此系统中，基于遗传编程的交易智能体负责从历史金融数据中提取可行的交易策略，并根据学到的策略在交易时输出交易信号。量子金融交易智能体和量子金融风控智能体则用于应对市场中的突发情况，如金融危机。实验结果表明，在2020年因新型冠状病毒导致的道琼斯工业平均指数暴跌的情况下，该系统相比买入并持有交易策略获得了超额收益。

The Design and Implementation of Multi-agent-based Quantum Trading System

B.H. Wu [1,*], C. H. Li [1]
Supervisor: Dr. Raymond S. T. Lee
[1] *Computer Science and Techonology, Division of Science and Technology, BNU-HKBU United International College*
**Corresponding student author. Tel: +86-137-1949-6908, E-mail: bowenbhwu@gmail.com*

Abstract

Artificial Intelligence (AI) programs developed for traders to trade automatically received significant attention in both the financial industry and academia since trader programs in the financial market have grown rapidly in recent decades. However, many popular AI-based program trading models experienced a “black box effect,” where the model may produce excellent results for trading but fail to explain how the model would behave in a certain way. Genetic programming (GP), on the other hand, can generate human-interpretable rules and predictable model behavior, but many studies have shown that the rules cannot generate an excess return over the straightforward buy and hold strategy. In this project, we designed a multi-agent-based quantitative trading system that combines GP with quantum finance. A GP-based trading agent in the proposed system extracts trading rules from historical financial data and yields trading signals based on the rules learned. Also, the quantum finance trading agent and quantum finance risk control agent are implemented to manage unseen market crashes. Statistical results show the system can generate excess returns over buy-and-hold trading strategies at the Dow Jones Industrial Average market crash caused by COVID-19 in 2020.
Keywords: genetic programming; quantum finance; multi-agent-based trading system; discovering trading rules; quantitative trading; risk control

Introduction

Genetic programming (GP) is an evolutionary algorithm with reasonable interpretability [1]. Unlike training or optimizing uninterpretable parameters in many machine learning and deep learning models, GP randomly generates human interpretable rules and optimizes the rule using genetic operators, including natural selection, crossover, and mutation, according to a fitness metric. Therefore, employing GP in the financial market to extract interpretable trading rules instead of leaving a single output with numerous incomprehensible parameters has more potential for being adopted by traders and provides insights into the financial market. However, studies presented in [2][3][4] show that the extracted rules using GP are hard to outperform the simpler buy-and-hold trading strategy, where traders purchase the product on the first day and keep it since then. One of the possible explanations for the phenomenon is that GP models tend to make risky decisions when the current market trend is not seen during training, like the market crash in the United States due to COVID-19 in 2020.

To minimize the risk in an investment, we need a way to measure whether the price drop belongs to daily oscillation or a severe market event. Quantum price levels (QPLs), similar to Fibonacci retracement in technical analysis, locate the support and resistance levels. However, using Fibonacci retracement to locate the support and resistance visually is prone to human error, and it can be difficult for computers. QPLs, on the other hand, are derived from quantum finance theory, and the calculation is based on conversion, revision, and new interpretation of quantum mechanical equations. By incorporating QPLs, we can find the resistance lines in the current market and use these quantum price levels to signal a potential bearish market.

Methdology

Genetic algorithm

Genetic programming (GP) is an extension of genetic algorithms. Instead of encoding the parameters into a chromosome, which is usually represented as a string, in genetic programming, the program is encoded into a parse tree. A parse tree contains the syntactic structure of a string defined by some context-free grammar.

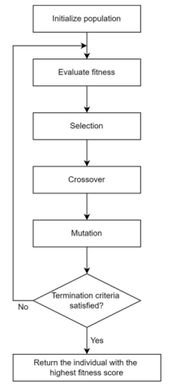

Figure 1: The Flow of Genetic Algorithm

Genetic programming

Genetic programming (GP) is an extension of genetic algorithms. Instead of encoding the parameters into a chromosome, which is usually represented as a string, in genetic programming, the program is encoded into a parse tree. A parse tree contains the syntactic structure of a string defined by some context-free grammar.

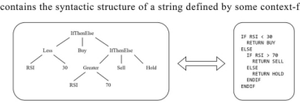

Figure 2: Example of GP

GP models are optimized using the genetic algorithm, which includes applying genetic operators on a set of parse trees using natural selection (fitness evaluation and discarding poorly performed individuals), crossover, and mutation, over a given number of generations. Fitness evaluation, which is a part of natural selection, is done by running the genetic programming model on a given problem and measuring its performance. The algorithm then discards individuals with poor performance. In the reproduction phase, two random surviving parse trees are selected to exchange part of their parse tree for every new parse tree (crossover). To introduce gene diversity into the population, mutation replaces part of the parse tree with a newly grown subtree.

Quantum Price Levels

Similar to Fibonacci retracement in technical analysis, quantum price levels locate the support and resistance levels according to historical market prices. According to Lee in [6], the price of a financial instrument is not only a scalar value in classical finance but also the intrinsic energy it possesses since the price movement is believed to be a consequence of all participants’ action dynamics in the financial market. In that case, the energy levels concept of an atom can be transformed to construct the idea of quantum finance energy levels (QFELs) that exist in every financial market as invisible energy levels. Quantum finance particles (QFPs) will remain stable without external stimuli such as financial events, index figure releases, and news. However, QFPs will “jump” to another energy level (i.e., QPLs) once there is a significant stimulus. The market maker then absorbs this stimulus, and QFPs will return to an equilibrium state at a new energy level, similar to energy levels in classical quantum mechanics.

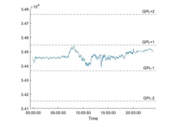

Figure 4: Daily oscillation on July 1, 2021

Figure 5: Major financial event on July 20, 2021

The Proposed System

In this study, we proposed the GP-QF trading system. In the system, GP generates trading rules from the training set, and QF is responsible for managing the risk involved in the investment. Quantum. The system contains three agents:

GP-based trading agent (GPBTA) extracts trading rules from training data by following the genetic algorithm procedures. The trading rules learned are used to generate ternary trading signals consisting of buy, hold, or sell at the start of every trading day.

Quantum finance risk control agent (QFRCA) monitors the minutely price on trading days. It will close a position and disables GPBTA if the market price falls below a given warning quantum price level (QPL) for one or more consecutive days (validation period), which indicates there are significant market events that could result in a potential bearish market. Similarly, if the market moves towards a favorable trend, it will enable GPBTA and QFTA. The agent’s parameters, including the warning QPL and the length of the validation period, are optimized using the genetic algorithm.

Quantum finance trading agent (QFTA): on the day GPBTA is activated. It will open a position if GPBTA has a position closed by QFRCA and GPBTA does not object (yield a sell signal). It will disable itself after making the decision.

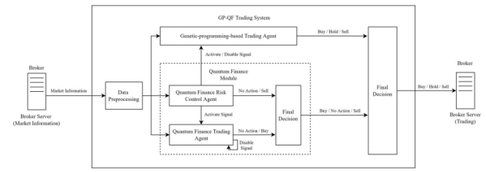

Figure 6: System architecutre

The system is trained in two stages. In the first stage, GPBTA is optimized to use trading rules that can generate a higher return without the assistance of QFRCA. Then, in the second stage, every model uses the best-performing GPBTA from the first stage. Each model has a different set of risk control parameters. Genetic algorithm is then applied to the model to find the best-performing model with the goal of generating a higher return while minimizing

Results and Discussion

The models are trained based on historical financial data from 2012 to 2019. The testing period covers the first trading day in 2020 to the last trading day in 2021. Experimental results on the test set showed that the GP-QF model outperforms the simpler buy and hold, MA, MACD, and RSI trading strategy in the training and test set. GP-QF trading system has significant improvements over GPBTA by correctly identifying the market crash period and drastically reducing MDD from -35% to -17% and increasing the rate of return by 10%.

Model	Return	MDD
GP-QF	**1.4006**	**-0.1677**
GPBTA	1.2647	-0.3479
Buy and Hold	1.2721	-0.3537
MA	1.2361	-0.0890
MACD	1.1181	-0.1030
RSI	1.2088	-0.3579

Table 1: Model comparison (test set)

Figure 7: Model comparison (test)

Conclusion

In this study, we proposed the GP-QF trading system. In the system, GP is employed to train on a set of randomly generates trading rules and are optimized to generate revenue. QPLs are used to locate the resistance lines of the current product and signal the system to handle potential crashes. By combining the two, we get a trading system that concerns both profitability and risk.

References

[1] J. R. Koza and J. R. Koza, Genetic Programming: On the Programming of Computers by Means of Natural Selection. MIT Press, 1992.
[2] C. Neely, P. Weller, and R. Dittmar, “Is Technical Analysis in the Foreign Exchange Market Profitable? A Genetic Programming Approach,” J. Financ. Quant. Anal., vol. 32, no. 4, pp. 405–426, Dec. 1997, doi: 10.2307/2331231.
[3] F. Allen and R. Karjalainen, “Using genetic algorithms to find technical trading rules,” J. Financ. Econ., p. 27, 1999.
[4] D. Lohpetch and D. Corne, “Outperforming Buy-and-Hold with Evolved Technical Trading Rules: Daily, Weekly and Monthly Trading,” in Applications of Evolutionary Computation, Berlin, Heidelberg, 2010, pp. 171–181. doi: 10.1007/978-3-642-12242-2_18.
[5] J. H. Holland, Adaptation in Natural and Artificial Systems: An Introductory Analysis with Applications to Biology, Control, and Artificial Intelligence. MIT Press, 1992.
[6] R. S. T. Lee, “Quantum Price Levels—Basic Theory and Numerical Computation Technique,” in Quantum Finance: Intelligent Forecast and Trading Systems, R. S. T. Lee, Ed. Singapore: Springer, 2020, pp. 89–118. doi: 10.1007/978-981-32-9796-8_5.

The implementation of autonomous driving system

C.L. Zhan
Supervisor: Dr. Z. Xuanyuan

自动驾驶系统的实现与部署

张楚梁
指导老师：轩辕哲博士

Abstract: Autonomous driving system is developing very fast nowadays. Although specific algorithms for target detection, location and trajectory planning have been studied intensively, there is urgent needs to build a testbed for autonomous driving systems to validate the proposed algorithms with real hardwares and softwares.

In this project, I realized the basic functions of the autonomous driving system with a four wheel robot platform, and illustrate the application of all kinds of algorithms involved. Firstly, I implemented the perception, planning and control modules based on the open source Autoware framework, and validated the algorithms required for scene recognition, path planning and vehicle control. Secondly, the system was deployed on the Lgsvl simulator to test whether the system function works normally. After that, I deploye the whole system to the real testing platform Autolabor_Pro1, and use lidar, camera and other sensors to build the environment maps, and finally test the whole autonomous driving system and functions in the real scenes. The results showed that we have successfully achieved all the target functions, and the vehicle can drive automatically in the real scene. The platform is readily usable as a testbed for future algorithm designs in autonomous driving technology.

摘要：目前，自动驾驶系统发展很快。尽管针对目标检测、定位和轨迹规划的具体算法已经得到了深入的研究，但迫切需要为自动驾驶系统搭建一个测试平台，用真正的硬件和软件验证所提出的算法。
在这个项目中，我用一个四轮机器人平台实现了自动驾驶系统的基本功能，并举例说明了各种算法的应用。首先，我们基于开源Autoware框架实现了定位、感知、规划和控制模块，并验证了场景识别、路径规划和车辆控制所需的算法。其次，将系统部署在Lgsvl模拟器上，测试系统功能是否正常工作。之后，我们将整个系统部署到真实的测试平台Autolabor_Pro1上，并使用激光雷达、摄像头等传感器构建环境地图，最后在真实场景中测试整个自动驾驶系统和功能。结果表明，我成功地实现了所有目标功能，并且车辆能够在真实场景中自动驾驶。该平台可作为未来自动驾驶技术算法设计的测试平台。

The implementation of autonomous driving system

C. L. Zhang[1]
Supervisor: Dr. Z. Xuanyuan

[1] Data Science Program, Division of Science and Technology, BNU-HKBU United International College
** Corresponding student author. Tel: +86-17689759989, E-mail: n830026152@mail.uic.edu.cn*

Abstract

Autonomous driving system is developing very fast nowadays. Although specific algorithms for target detection, location and trajectory planning have been studied intensively, there is urgent needs to build a testbed for autonomous driving systems to validate the proposed algorithms with real hardwares and softwares.

In this project, we realized the basic functions of the autonomous driving system with a four wheel robot platform, and illustrate the application of all kinds of algorithms involved. Firstly, we implemented the perception, planning and control modules based on the open source Autoware framework, and validated the algorithms required for scene recognition, path planning and vehicle control. Secondly, the system was deployed on the Lgsvl simulator to test whether the system function works normally. After that, we deploye the whole system to the real testing platform Autolabor_Pro1, and use lidar, camera and other sensors to build the environment maps, and finally test the whole autonomous driving system and functions in the real scenes. The results showed that we have successfully achieved all the target functions, and the vehicle can drive automatically in the real scene. The platform is readily usable as a testbed for future algorithm designs in autonomous driving technology.

Keywords: *Autonomous driving system, Autoware, LGSVL, Robot Operating System, Localization, Perception, Planning, Control*

Introduction

From the perspective of the future development direction of the world industry, autonomous driving technology has great potential in improving traffic safety and traffic efficiency, and will greatly change the future traffic mode. It is a cutting-edge research hotspot in the field of intelligent transportation at present and in the future, and is regarded as a new strategic highland by major developed countries in the world. In the national strategic action plan of Made in China 2025, China also clearly puts forward that "by 2025, China should master the overall technology and key technologies of autonomous driving and basically complete the transformation and upgrading of the automobile industry"[4].

Now various vehicle manufacturers and driverless solution providers are emerging in endlessly. For example, Tesla, Baidu Apollo, etc. are constantly promoting autonomous vehicles.

Related Work

Robot operating system (ROS) is a general framework for robot software development. On a common platform, developers can merge various software released by other developers and speed up development by reusing them. ROS provides a rich variety of libraries and tools for robot software development. It uses a message passing mechanism based on topic publishing and subscription in the inter module connection / cooperation framework.

Based on the open source software framework of autonomous driving based on ROS platform, autoware.ai. The source code of autoware.ai is hosted in gitlab. The core capabilities of Autoware system can be roughly divided into five categories, namely Sensing, Localization, Perception, Planning and Control. The interaction between these capabilities and the interaction between vehicles and the environment through multiple sensors realize autonomous driving. Similar to Apollo, the nodes in each module of Autoware run independently based on ROS. Each module node publishes and subscribes to certain topics. Subscribed topics are used as data input and published topics are used as data output.

Overall system framework

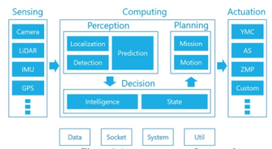

Figure 1 Autoware system framework

The core capabilities of Autoware system can be roughly divided into five categories, namely Sensing, Localization, Perception, Planning and Control. The interaction between these capabilities and the interaction between vehicles and the environment through multiple sensors realize autonomous driving. The nodes in each module of Autoware run independently based on ROS. Each module node publishes and subscribes to certain topics. Subscribed topics are used as data input and published topics are used as data output. Each module has different ROS nodes, as shown in the figure below.

Figure 2 Each module node of autoware

Function description & Demo

Based on autoware system, I built the vehicle Sensing, Localization, Perception, Planning and Control module. This is my system architecture, on which are the nodes in Autoware. Figure 3 shows all the nodes included in my system.

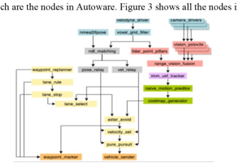

Figure 3

Each module node publishes and subscribes to certain topics. Subscribed topics are used as data input and published topics are used as data output.

In the process of driving, the autonomous vehicle needs to provide its own accurate position on the lane for decision-making and planning. Based on 3D high-precision map data and normal distribution transformation (NDT) algorithm, through the process of matching various types of sensors, such as GNSS, IMU, vehicle camera, lidar, etc., with the data in the high-precision map, we can accurately obtain our position in the current space.

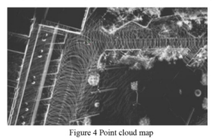

Figure 4 Point cloud map

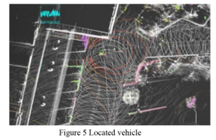

Figure 5 Located vehicle

The perception module is the link between the vehicle and the environment. It further processes the perceived information by sensing the surrounding environment, scene objectives and other information, so as to provide a basic basis for planning. Representative methods include RCNN, SSD and Yolo. Figure 26 is a visual result of object detection using yolov3.

Figure 6 Object detection

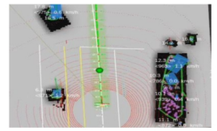

Figure 7 Autoware obstacle map

The autonomous driving decision planning module integrates the perception of the environment and the information of the vehicle, determines the behavior and trajectory of the vehicle, and guides the control module to control the vehicle. I will apply the A * algorithm based on graph search in avoiding obstacles. The control stack generates control signals to drive the vehicle to follow the vehicle dynamic trajectory. The control commands of tire angular speed and linear speed are processed and issued based on the principle of pure pursuit algorithm. In Figures 7 to 10, the green path in the visual interface is the path planned by the decision planning module.

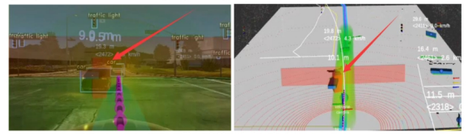

Figure 8 Obstacle detection

In Figure 8 and Figure 9, we can see that other vehicles (obstacles) appear in front of the vehicle, which is visualized as a red rectangle on the visualization interface. As the vehicle perception module detects the obstacles in front, the planning module starts to re plan the path to bypass the obstacles in front. We can see that the green path in Figure 9 has changed. At this time, the car starts to turn to avoid the obstacles in front.

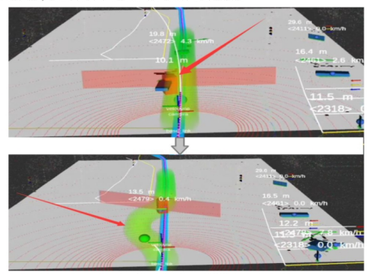

Figure 9 Obstacle avoidance

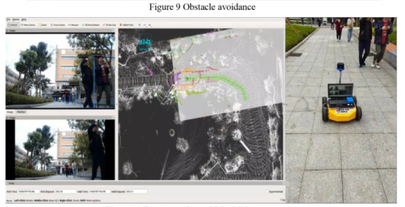

Figure 10 Demonstration vehicle driving on campus

References

- [1] Tas, Ömer & Kuhnt, Florian & Zöllner, J. & Stiller, Christoph. (2016). Functional System Architectures towards Fully Automated Driving. 10.1109/IVS.2016.7535402.
- [2] GitHub-Computing Platforms Federated Laboratory. Autoware-Manuals[DB/OL]. [2020] https://github.com/CPFL/Autoware.Manuals.
- [3] Autoware-AI, "Readme document of autoware.ai github," Autoware, 19 June 2020. [Online]. Available: https://github.com/Autoware-AI/autoware.ai/wiki/Overview. [Accessed 25 June 2020].
- [4] SamSung, "github repository of LGSVL simulator," 28 May 2020. [Online]. Available: https://github.com/lgsvl/simulator. [Accessed 13 July 2020].
- [5] Pendleton, Scott et al. "Perception, Planning, Control, and Coordination for Autonomous Vehicles." Machines 5, 1 (February2017): 6 © 2017 The Author(s)

Lab Simulation of Heavy Metal Adsorption by Microplastics in Single and Mixed Metal Solutions

L. S. Fu, Y. N. Wang
Supervisor: Prof. H. D. Ruan

实验室模拟微塑料在单一及混合金属溶液中对重金属的吸附

付龙山、王彦宁
指导老师：阮华达教授

Abstract: Microplastics refer to plastic fragments with a particle size of less than 5 millimeters, and they attract scientists' attention all over the world as an emerging pollutant. Microplastics have a large specific surface area. It has been proved that microplastics in the environment can adsorb other pollutants such as heavy metals, and show a synergistic toxic effect on the ecosystem. In this project, an 84-hours laboratory simulation experiment was conducted to compare the adsorption of four heavy metals (Cu, Zn, Cd, Pb) by three microplastics (PVC, PS, PP) in four single metal solutions to a solution with the coexistence of four heavy metals. The concentrations of metal ions remaining in the solution were detected by ICP-MS. In both single metal solutions and coexisting solution, the adsorption capacities of the three types of microplastics were in an order of Pb > Cu > Cd > Zn. PVC microplastics showed the highest adsorption capacity while PS and PP shared a similar adsorption tendency on the four selected metals. Rather than adsorption happened all the time, desorption phenomenon can be observed during the 84h period of time. For Cu, Zn and Cd, the adsorption capacities of these three microplastics had a slight increment after desorption. Pb was adsorbed more rapidly than the other three heavy metals. A surprise finding was that, each microplastics showed a higher adsorption capacity to heavy metals in mono-metallic solutions than in mixed metal solution, indicating that competition occurred among different heavy metal ions when they moved towards the adsorption sites of microplastics.

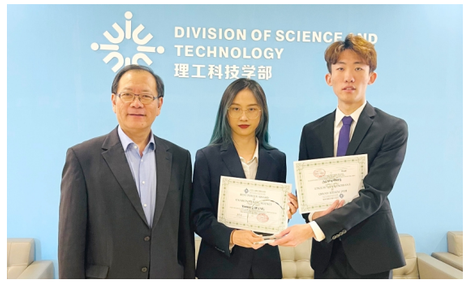

摘要：微塑料是粒径小于5毫米的塑料碎片，它作为一种新兴污染物，已成为科学家们广泛研究的对象。微塑料有比较大的比表面积。环境中的微塑料已被证实能吸附其他污染物（如：重金属），并且对生态系统表现出协同毒性作用。本研究通过周期为84小时的模拟实验，比较了PP（聚丙烯）、PS（聚苯乙烯）和PVC（聚氯乙烯）三种微塑料在铜、锌、镉、铅四种金属的单一金属溶液及其四种金属共存的溶液中对Cu2+、Zn2+、Cd2+、Pb2+四种重金属离子的吸附量差异。在单一金属溶液及混合金属溶液中，三种被研究的微塑料对重金属离子吸附能力的顺序都表现为：Pb2+ > Cu2+ > Cd2+ > Zn2+；其中，Pb2+能在短时间内被快速吸附并达到吸附动态平衡状态。PVC对重金属离子的吸附能力最强，PS和PP对这四种金属的吸附量有相似的吸附趋势。在84小时内，除了吸附现象，解附现象也在三种微塑料上有所体现，且微塑料对Cu2+、Zn2+、Cd2+的吸附能力在解附后均有较小的提升。此外，三种微塑料在单一金属溶液中对四种金属都有更高的吸附量，这表明在混合金属溶液中，微塑料对不同重金属离子存在竞争吸附作用。

Lab Simulation of Heavy Metal Adsorption by Microplastics in Single Metal Solution and Mixed Metal Solution

L.S. Fu [*1], Y.N. Wang [*1]
Supervisor: Prof. H.D. Ruan
[1]*Environmental Science Program, Division of Science and Technology, BNU-HKBU United International College*
**Longshan Fu. Tel: +86-13287321183, E-mail:* n830004003@mail.uic.edu.cn
**Yanning Wang. Tel: +86-13302213498, E-mail:* n830004029@mail.uic.edu.cn

Introduction

Microplastics

- Diameter < 5-mm
- Large specific surface area, refractory degradation, wide migration range.
- Ability to adsorb other pollutants, e.g., heavy metals.

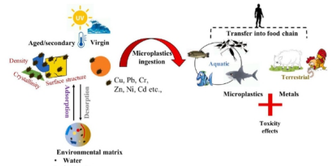

Figure 1: Illustration showing interaction of metals with microplastics and their transfer pathways into food chain in the environment (Kutralam-Muniasamy et al., 2021).

Research Significance

Various researches have been conducted to find out the adsorption mechanism between microplastcis and single heavy metal in aqueous. However, few studies focus on the adsorption of heavy metals in single-metal and multi-metal coexisting systems simultaneously. Since the nature acts as a huge container holding lots of heavy metals, further study on the adsorption behaviour in mixed metal solution is necessary to discover the co-toxicity between these two kinds of pollutants on ecological health.

Aim

To discover the adsorption capacities between microplastics and heavy metals in both single metal solution and mixed metal solution.

Objectives

- To figure out adsorption, desorption and adsorption competition phenomena in this project.
- To figure out the adsorption capacities of the three types of studied microplastics in different time.
- To figure out different adsorption capacities of microplastics to heavy metals between mono-metallic solutions and mixed metal solutions.

Methodology

- Materials

Microplastics:
PVC, PS, PP
- Specification: 300-μm
- 0.1000 g for each sample

Heavy metals:
Cu, Zn, Cd, Pb
- Chemical valance: +2
- 1 ppm for each sample

- Experimental Procedure

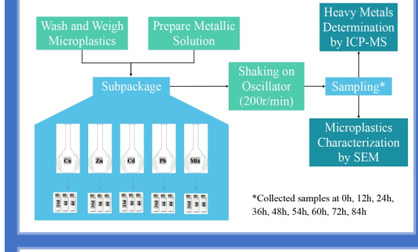

*Collected samples at 0h, 12h, 24h, 36h, 48h, 54h, 60h, 72h, 84h

Results and Discussion

Characterization of Microplastics

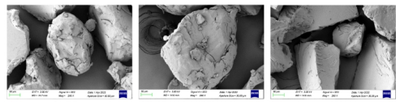

(a) PS (b) PP (c) PVC

Figure 2: These three graphs are SEM images of the microplastics surface morphology of pristine PS, PP and PVC.

Surface properties:
- PS and PP: Rough, ball-shape.
- PVC: Smooth, distinct edge and corner.

Adsorption Analysis of Microplastics

- **In Mono-metallic Solution**
- **In Mixture**

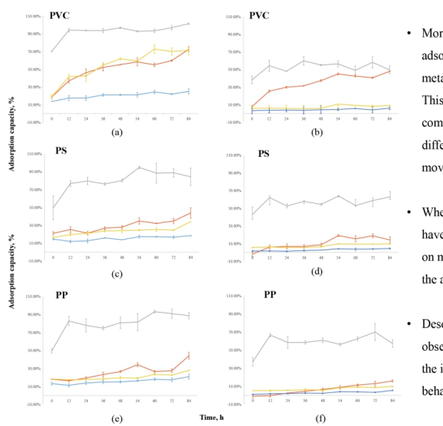

Figure 3: (a) ~ (f) show the adsorption capacity variation of PVC, PS and PP within 84-h.

- More Cu, Zn, Cd and Pb can be adsorbed by microplastics in mono-metallic solution than in mixture. This illustrates that adsorption competition occurred among different heavy metals when they moved towards microplastics.
- When four metal ions coexist, they have different affinity to active site on microplastics, which determined the adsorption order.
- Desorption phenomenon can be observed in all situation, showing the instability of the adsorption behavior of microplastics.

Total Adsorption Capacity in Mixed-metallic Solution

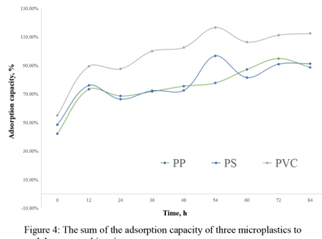

Figure 4: The sum of the adsorption capacity of three microplastics to each heavy metal in mixture.

Because PP and PS microplastic particles have similar surface their adsorption capacities are almost the same. Pproperties (Figure 1 a and b), PVC has the strongest adsorption capacity to heavy metals due to the functional group (-Cl).

PVC	PS	PP
$-(CH_2\text{-}CHCl)_n-$	$-(C_8H_8)_n-$	$-(C_3H_6)_n-$

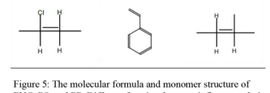

Figure 5: The molecular formula and monomer structure of PVC, PS, and PP. Different functional groups influence polarity, electrostatic force, etc.

Conclusion

- The adsorption capacities of the three types of microplastics: Pb > Cu > Cd > Zn.
- The adsorption capacity of PVC was the highest; while that of PS and PP are similar.
- Each microplastic showed a higher adsorption capacity to heavy metals in mono-metallic solutions than in mixed metal solutions, indicating that competition occurred among different heavy metal ions.

Key References
Brennecke, D., Duarte, B., Paiva, F., Caçador, I., & Canning-Clode, J. (2016). Microplastics as vector for heavy metal contamination from the marine environment. *Estuarine, Coastal and Shelf Science*, 178, 189-195. doi:10.1016/j.ecss.2015.12.003
Gao, F., Li, J., Sun, C., Zhang, L., Jiang, F., Cao, W., & Zheng, L. (2019). Study on the capability and characteristics of heavy metals enriched on microplastics in marine environment. *Marine Pollution Bulletin*, 144, 61-67.
Godoy, V., Blázquez, G., Calero, M., Quesada, L., & Martín-Lara, M. A. (2019). The potential of microplastics as carriers of metals. *Environmental Pollution (1987)*, 255(Pt 3), 113363. doi:10.1016/j.envpol.2019.113363
Oz, N., Kadizade, G., & Yurtsever, M. (2019). Investigation of heavy metal adsorption on microplastics. *Applied Ecology and Environmental Research*, 17(4), 7301-7310. doi:10.15666/aeer/1704_73017310

Night image enhancement algorithm

*Z. Y. Liu C. C. Lu
Supervisor: Dr. W. Zhang

夜间图像增强算法

刘子怡、陆程程
指导老师：张未博士

Abstract: Due to insufficient or uneven illumination at night, the captured images usually have low contrast, visibility and suffer from poor human eyes observation and information loss. The main purpose of nighttime image enhancement is to improve image contrast and brightness. This paper analyses the enhancement algorithms based on histogram equalization, Retinex image processing, and some merged algorithms. Furthermore, the advantages and disadvantages of these algorithms are summarized. An algorithm called WRCLAHE is proposed, which is based on wavelet transform, histogram equalization, and Retinex, to avoid the problems of detail loss, whitening, and noise being amplified after nighttime image enhancement. The method firstly denoises the image with wavelet transform, then processes the denoised image with adaptive histogram equalization and Retinex, respectively, and finally fuses the processed image with wavelet transform image fusion method based on region characteristic measurement. Experimental results of processing night images show that the visual effect of the image enhanced by the algorithm is further enhanced, the image has more detailed features, and the problem of image halo is solved at the same time. In addition, the objective evaluation metrics of the WRCLAHE algorithm show a great result of this method in image enhancement. Therefore, through our experiment, we conclude that the WRCLAHE algorithm has a good effect on the color restoration and color fidelity of low-illumination images.

摘要：由于夜间光照不足或不均匀，所拍摄的图像通常存在对比度低，能见度低，人眼观察效果差，信息丢失等问题。夜间图像增强的主要目的是提高图像的对比度和亮度。本文分析了基于直方图均衡、Retinex及其衍生算法的增强算法。此外，还总结了这些算法的优点和缺点。本文提出了一种名为WRCLAHE的算法，该算法基于小波变换、直方图均衡和Retinex算法，避免了夜间图像增强后细节损失、曝光和噪声被放大的问题。该方法首先用小波变换对图像进行去噪，然后分别用自适应直方图均衡和Retinex算法处理去噪后的图像，最后用基于区域特征测量的小波变换图像融合方法，对处理后的图像进行融合。实验结果表明，通过该算法增强的夜间图像，图像的视觉效果进一步提高，且特征更加细致，同时解决了图像光晕的问题。此外，WRCLAHE算法的客观评价指标显示了该方法在图像增强方面的巨大效果。因此，通过实验，我们得出结论：WRCLAHE算法对低照度图像的色彩还原和色彩保真具有良好的效果。

Night image enhancement algorithm

Z.Y. Liu 1 * / C.C. Lu 2
Supervisor: Dr. W. Zhang
Financial Mathematics Program, Division of Science and Technology, BNU-HKBU United International College
** Corresponding student author. Tel: +86-18773113824, E-mail: n830018047@mail.uic.edu.cn*

Abstract

Due to insufficient or uneven illumination at night, the captured images usually have low contrast, visibility and suffer from poor human eyes observation and information loss. The main purpose of nighttime image enhancement is to improve image contrast and brightness. This paper analyses the enhancement algorithms based on histogram equalization, Retinex, and their derivative algorithms. Furthermore, the advantages and disadvantages of these algorithms are summarized. An algorithm called WRCLAHE is proposed, which is based on wavelet transform, histogram equalization, and Retinex, to avoid the problems of detail loss, whitening, and noise being amplified after nighttime image enhancement. The method first denoises the image with wavelet transform, then processes the denoised image with adaptive histogram equalization and Retinex, respectively, and finally fuses the processed image with wavelet transform image fusion method based on region characteristic measurement. Experimental results of processing night images show that the visual effect of the image enhanced by the algorithm is further enhanced, the image has more detailed features, and the problem of image halo is solved at the same time. In addition, the objective evaluation metrics of the WRCLAHE algorithm show a great result of this method in image enhancement. Therefore, through our experiment, we conclude that the WRCLAHE algorithm has a good effect on the color restoration and color fidelity of low-illumination images.

Introduction of Histogram Equalization

Basic steps of histogram equalization

- Calculate the gray histogram h(k) and the total number of pixels N
- Calculate the Cumulative Distribution Frequency of gray level
- Restore image grayscale values

Original histogram　　Histogram after equalization

Contrast Limited Adjust Histogram Equalization

- Partition
- Adjust the gray histogram
- Histogram Equalization
- Pixel gray value reconstruction

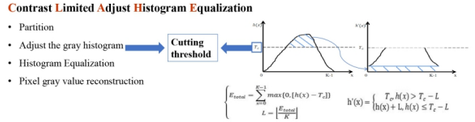

Histogram Equalization Experiment Results

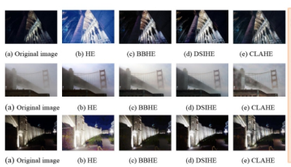

Summary of Histogram Equalization

CLAHE preforms best

Advantage of CLAHE algorithm:

1. Improve the contrast
2. High color fidelity
3. Keep details

Disadvantages of CLAHE algorithm:

1. Can not identify all the objects

Introduction of Wavelet transform

The wavelet transform of an image is the **convolution** of the rows and columns of the image with a low-pass filter and a high-pass filter

$$DWT(scale, translation) = \int_0^{+} f(t)\psi(2^j, 2^j m, time)dt$$

Mallat algorithm: DWT = using filters

Basic steps of on image denoising

- Perform DWT, obtain the corresponding coefficients C
- Thresholding coefficients C, obtain the estimated wavelet coefficients C*
- Perform Inverse DWT on C*

Wavelet Denoising Experiment Results

Introduction of Retinex Algorithm

Retinex algorithm is used to simulate the human visual system. The theory is based on the idea that in the case of uniform illumination, the original image $S(x, y)$ is the combination of the reflection component $R(x, y)$ and the illumination component $L(x, y)$.

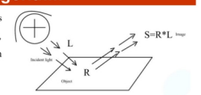

Single-scale Retinex algorithm/SSR

Land proposed the central peripheral Retinex algorithm, which has a small number of parameters and is easy to implement. The core idea of the algorithm based on the central peripheral function is to estimate the illuminance component with a Gaussian kernel function.

$$S(x,y) = R(x,y) \cdot L(x,y)$$
$$L(x,y) = F(x,y) * S(x,y)$$

$*$ represents convolution operation, which is an effective method for extracting image features; $F(x,y)$ represents Gaussian kernel function, the expression is:

$$F(x,y) = \lambda \exp\left(-\frac{x^2+y^2}{c^2}\right)$$

c is the Gaussian scale constant, and its function is to control the range of the neighborhood. λ is the attribution factor, which satisfies the following formula:

$$\iint F(x,y)dxdy = 1$$

In order to facilitate the conversion of equation to the logarithmic domain.

$$r(x,y) = \log R(x,y) = \log S(x,y) - \log[F(x,y) * S(x,y)]$$
$$R(x,y) = exp(r(x,y))$$

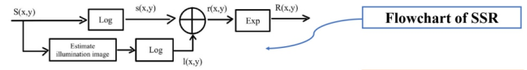

Single-scale Retinex Experimental Eesults

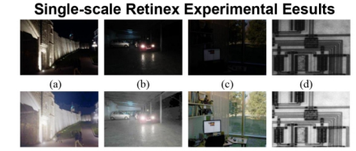

Summary of SSR algorithm

Advantages:

1. Identify objects in the dark
2. Enhance image brightness
3. Improve image contrast
4. High color fidelity

Disadvantages:

1. Halo and overexposure problems
2. Lose some details

Innovation of night image fusion algorithm

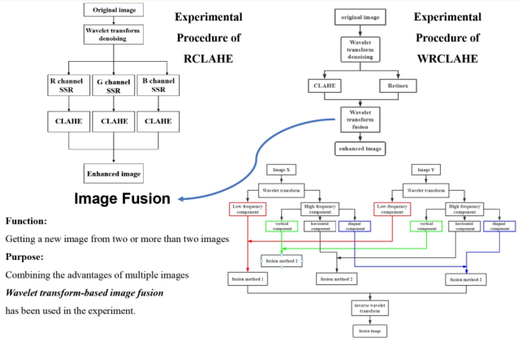

Function:

Getting a new image from two or more than two images

Purpose:

Combining the advantages of multiple images

Wavelet transform-based image fusion

has been used in the experiment.

Conclusion and Total Experimental Results

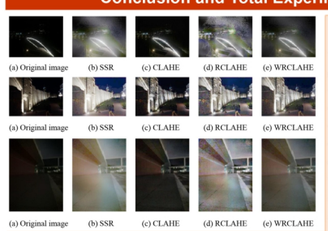

Conclusion

WRCLAHE algorithm has shown good performance in:

- Detail reservation;
- Color fidelity;
- Improvement of image contrast;
- Improvement of overall brightness.

Compared with SSR:

WRCLAHE solve the problem of exposure effect and color distortion which caused by the comparative light source in the dark image.

Compared with CLAHE: The brightness and detail reservation of the processed image by WRCLAHE are much better.

Compared with RCLAHE: The color transition of the picture processed by WRCLAHE is more natural compared with RCLAHE.

Reference

[1] Bai Huanghuang. (2017). Nighttime image defogging based on the theory of retinex and dark channel prior. Laser & Optoelectronics Progress, 54(4), 041002.
[2] R Hummel. (1975). Image Enhancement by Histogram Transformation.
[3] Artur, Bull, D. R. , Hill, P. R. , & Achim, A. M. . (2013). Automatic contrast enhancement of low-light images based on local statistics of wavelet coefficients. Digital Signal Processing, 23(6), 1856-1866.
[4] Land, E. H. . (1978). The retinex theory of color vision. Scientific American, 237(6), 108-128.
[5] Deng A, Wu Z, Yang X, et al. Image fusion algorithm based on second-generation Curvelet transformation and region matching degree [J]. *Computer Science*, 2012(6) : 513 - 515.
[6] Guo, Z. Q. . (2005). Wavelet transform image fusion based on regional features. Journal of Wuhan University of Technology.
[7] Gonzalez, R. C. , & Woods, R. E. . (1980). Digital image processing. IEEE Transactions on Acoustics Speech and Signal Processing, 28(4), 484-486.

Biodegradable, pH Sensitive Micelle for the Co-delivery of Calycosin-7-O-β-D-glucoside and Cis-platin

Z. R. Mao
Supervisor: Dr. Y. Wang

基于葡聚糖和聚乳酸的生物可降解的pH响应胶束用于抗癌药物的靶向递送

毛泽睿
指导老师：王娅博士

Abstract: Currently, cancer is a health problem worldwide. As the most commonly used treatment for cancer, chemotherapy has low drug efficiency and significant side effects which lead to sufferings to patients due to the lack of selectivity. Targeted drug delivery systems can effectively improve the efficiency and reduce the side effects of drugs. It has been proven that synergistic administration of cis-platin and calycosin-7-O-β-D-glucoside could enhance the efficiency and reduce the side effects of cis-platin. This project aims to develop a fully biodegradable, pH sensitive micelle carrier based on dextran and polylactic acid for the co-delivery of calycosin-7-O-β-D-glucoside and cis-platin in order to further improve the anticancer effect and reduce the side effect of cis-platin. To prepare the micelle carrier, on one hand, the hydroxide groups on dextran were first modified with carboxymethyl groups, the degree of substitution (DS) was 171%. The carboxymethyl groups were then modified with amine groups, DS was 30%. On the other hand, polylactic acid (PLA) was synthesized by end functionalized ring open polymerization with aldehyde group at the end, the average molecular weight was 10,489 Da. Dextran-poly (lactic acid) micelle was fabricated via the generation of pH sensitive hydrazone bonds with amine groups from dextran and aldehyde groups from PLA. The average size of micelle was 355.4 nm measured by dynamic light scattering (DLS). The formation of hydrazone bonds enables the micelle to disassemble in acidic environments such as cancer sites and selectively release the encapsulated cis-platin and calycosin-7-O-β-D-glucoside to achieve targeted therapy.

摘要：癌症目前是一个全球性的健康问题，传统的化疗作为治疗癌症最常用的手段，因缺乏选择性，治疗效率低且副作用大。具有靶向性的药物递送系统可有效提高药效并降低药物的副作用。研究表明，顺铂与毛蕊异黄酮葡萄糖苷的联合使用可提高顺铂的疗效并减少其副作用。本研究项目将设计并合成一种生物可降解，pH敏感的葡聚糖-聚乳酸胶束载体，实现对毛蕊异黄酮葡萄糖苷和顺铂的协同传递，以进一步提高顺铂的抗癌效果。为制备胶束，一方面葡聚糖上的氢氧基首先被羧甲基修饰，取代度为171%；然后进一步用胺基修饰羧甲基，取代度为30%。另一方面，通过端基功能化开环聚合合成聚乳酸，其平均分子量为10489 Da。最后，通过pH敏感的腙键将葡聚糖上的胺基与聚乳酸上的醛基结合制备葡聚糖-聚乳酸胶束。利用动态光散射（DLS）测得所制备的胶束平均粒径为355.4纳米。腙键的形成使得该胶束可以在微酸性环境如癌症部位解散，高选择性地释放其中包载的顺铂与毛蕊异黄酮葡萄糖苷药物，实现靶向治疗。

Biodegradable, pH Sensitive Micelle Based on Dextran and Polylactic Acid as Delivery System for Anticancer Drugs

Z.R. Mao *
Supervisor: Dr. Y. Wang
Food Science and Technology Program, Division of Science and Technology, BNU-HKBU United International College
**** Corresponding student author. Tel: +86-13719389865, E-mail: n830013022@mail.uic.edu.cn***

Abstract

Currently, cancer is a health problem worldwide. As the most commonly used treatment for cancer, chemotherapy could lead to suffering to patients due to the low selectivity of drugs. Different kinds of drug delivery systems have been developed in order to reduce the side effects of drugs. This project provides a new idea of drug delivery system, in which biodegradable dextran and polylactic acid are utilized to prepare a pH sensitive nano micelle. The hydroxide groups on dextran were first modified with carboxymethyl groups, the degree of substitution (DS) was tested to be 171%. The carboxymethyl groups were then modified with amine groups, DS was tested to be 30%. Polylactic acid (PLA) was synthesized by end functionalized ring open polymerization with aldehyde group at the end. Dextran-poly (lactic acid) micelle was fabricated via the generation of pH sensitive hydrazone bonds between amine groups from dextran and aldehyde groups from PLA in the mixture of water and tetrahydrofuran. The average particle size of micelle was 355.4 nm measured by dynamic light scattering (DLS). The formation of hydrazone bond ensures the sensitivity of the micelle to pH change which could be potentially applied for selective cancer treatment.

Keywords: *Biodegradability, pH sensitivity, drug delivery system, micelle.*

Introduction

Cancer is now the second leading cause of morbidity and mortality worldwide, which has killed about 10 million people each year, or led to one in six deaths. Currently, among different treatments to cancer, chemotherapy is the most common used method. However, due to the less selectiveness of chemotherapeutic drugs, they could cause damage to normal cells while killing tumor cells, which make patients suffer from it.

To improve the efficiency of drugs, drug delivery system that based on small particles have been developed, micelle was one of them. Micelle is kind of polymer molecule with hydrophilic and hydrophobic ends, under the influence of intermolecular forces in aqueous solvent, the polymer molecules will gather together to form the micelles. With the micelles, the selectiveness of drugs could be improved and the side effects could be reduced.

The purpose of this research is to take the advantage of excellent biodegradability and biocompatibility of dextran and polylactic acid, to synthesize a novel micelle as the platform for encapsulating hydrophobic chemotherapy drugs such as *cis*-platinum and doxorubicin (DOX).

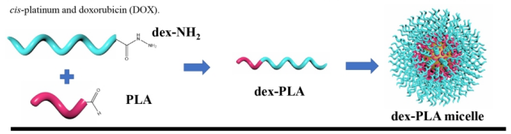

Methods

(a) Synthesis and characterization of carboxymethyl modified dextran (CMD)

(b) Synthesis and characterization of amine modified dextran (dex-NH_2)

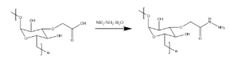

(c) Synthesis and characterization of aldehyde end functionalized polylactic acid (PLA)

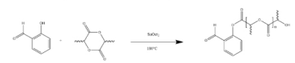

(d) Synthesis and characterization of dex-PLA micelle

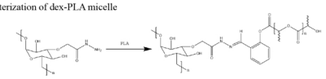

Results and Discussion

(a) Characterization of CMD

The functional groups of dextran and CMD were characterized by FT-IR and the spectra were shown in Figure 1. CMD has two new peaks at 1585 cm^{-1} and 1719 cm^{-1}, replaced the peak at 1645 cm^{-1} in dextran. These changes in the functional groups indicated that some hydroxyl groups in the dextran molecules have been replaced by carboxyl groups, which confirmed the successful modification.

The molecular structure of CMD was then characterized by ^1H NMR and the spectrum was shown in Figure 2. Ratio of peak area between peak 7 and peak 1 was 1.7 : 1, this result means that there was average 1.7 carboxymethyl group on each ring of the glucose unit, confirmed that the carboxymethyl groups were successfully incorporated onto the backbone of dextran.

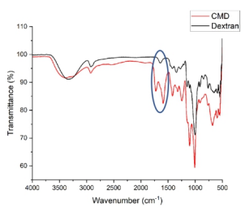

Figure 1. Infrared spectra of dextran and CMD.

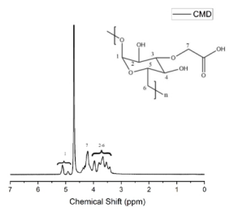

Figure 2. ^1H NMR spectrum of CMD.

(b) Characterization of dex-NH_2

The functional groups of dex-NH_2 were identified by FT-IR spectra as shown in Figure 3. The peak at 1582 cm^{-1} in CMD, was replaced by the two peaks at 1585 cm^{-1} and 1719 cm^{-1} in dex-NH_2. Changes in peaks primarily indicated the carboxymethyl groups been replaced by amine groups after the reaction with hydrazine hydrate.

The molecular structure of dex-NH_2 was then characterized by ^1H NMR and the spectrum was shown in Figure 4. The peak at 4.1 ppm represented the hydrogens at acetic acid structure and peak at 2.8 ppm region represented the amino group on the dextran structure. This result means there was average 0.3 amine group on each ring of the glucose unit, confirming that the amine groups were successfully incorporated onto the backbone of dextran.

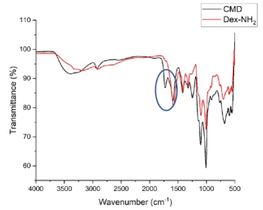

Figure 3. Infrared spectra of CMD and dex-NH_2.

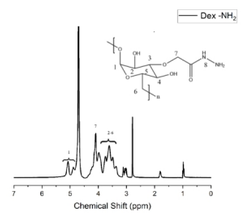

Figure 4. ^1H NMR spectrum of dex-NH_2.

(c) Characterization of PLA

The functional groups of PLA was identified by FT-IR spectra (Figure 5) and compared with the literature. The peaks at 2922cm^{-1}, 1747 cm^{-1}, 1453 cm^{-1}, 1381 cm^{-1}, 1180 cm^{-1}, 1080 cm^{-1}, and 754 cm^{-1} were corresponding to the peaks in the reference, which indicated the successful synthesis of PLA.

The molecular structure of PLA was then characterized by ^1H NMR and the spectrum was shown in Figure 6. The peak at 1.6 ppm region was due to the CH_3 structure and the peak at 5.2 ppm region was due to the CH structure in PLA, respectively. The peak area ratio between CH and CH_3 was 1:3, which was the same with the theoretical ratio in PLA, indicating the successful synthesis of PLA.

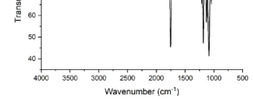

Figure 5. Infrared spectrum of PLA.

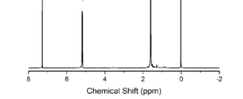

Figure 6. ^1H NMR spectrum of PLA.

(d) Characterization of dex-PLA micelle

The functional groups of micelle was first identified by FT-IR spectra as shown in Figure 7. The changes in peak at 1750cm^{-1} represented the loss of amine groups in the structure, which indicated the formation of micelle.

The particle size of the micelle was measured by dynamic light scattering (DLS) with concentration of 15 mg/mL. As shown in Figure 8, the average particle size of the micelles was 355.4 nm.

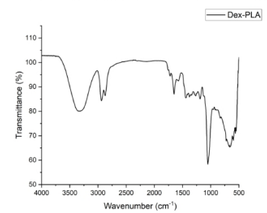

Figure 7. Infrared spectra of dex-PLA micelle.

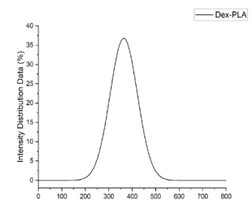

Figure 8. Micelle particle size distribution.

Conclusion

In this project, dextran was modified by carboxymethyl groups and then converted to amine groups. PLA was synthesized by polymerization of L-lactide. pH sensitive micelles were synthesized by the reaction between amine groups on dextran and aldehyde groups on PLA. The results from FT-IR, ^1H NMR and DLS proved that CMD, dex-NH_2, PLA and micelle were synthesized successfully, the average particle size of micelle was 355.4 nm. The results also proved that the synthesis of biodegradable micelle composed with dextran and PLA was feasible. With the pH sensitive hydrazone bonds, micelles could remain stable under normal physiological conditions and disassemble under acidic conditions to achieve targeted drug release for cancer therapy.

References

Icart, L. P., Fernandes, E., Aguero, L., Cuesta, M. Z., Silva, D. Z., Rodriguez-Fernandez, D. E., et al. (2017, 1). End Functionalization by Ring Opening Polymerizatoin: Influence of Reaction Conditions on Syntheses of End Functionalized Poly(lactic Acid). *Journal of the Brazilian Chemical Society*, pp. 1-10.

Wang, Y., Jia, H.-Z., Han, K., Zhuo, R.-X., & Zhang, X.-Z. (2013, 5 9). Theranostic magnetic nanoparticles for efficient capture and in situ chemotherapy of circulating tumor cells. *Journal of Materials Chemistry B*, pp. 1-9.

Extended Kalman-Particle Filter-based Phase Noise Compensation for CO-OFDM Systems

H. Y. Deng
Supervisor: Dr. X.W. Du

基于扩展卡尔曼-粒子滤波器的CO-OFDM系统的相位噪声补偿

邓惠匀
指导老师：杜新炜博士

Abstract: Coherent optical orthogonal frequency division multiplexing (CO-OFDM) combines the advantages of orthogonal frequency-division multiplexing, coherent detection and optical communication technologies, which becomes a promising technology for next-generation optical long-haul broadband communications. It has the merits of high spectral efficiency, receiving sensitivity and dispersion tolerance. However, CO-OFDM has the longer symbol duration compared to a single carrier system, that's why the coherent optical orthogonal frequency-division multiplexing (CO-OFDM) system is more sensitive to the linear phase noise (LPN) than that of the single carrier system. This paper proposes to compensate the LPN in a real-time and dynamic manner based on the extended Kalman-particle filter (EKPF). The phase noise estimation performance converge to the steady state by utilizing a pilot OFDM symbol, and then decision feedback algorithm is applied for further estimation and detection. Simulations are carried out through the dynamic tracking error and BER performance comparison with the conventional Bayesian filters in a 16-QAM 100 Gbps CO-OFDM system. Simulations results show that the proposed algorithm can achieve more accurate phase estimation and BER performance compared to the conventional Bayesian filters. So, EKPF combines the advantages of EKF and PF, which can provide an accurate estimate of time-domain phase noise with only a small number of particles.

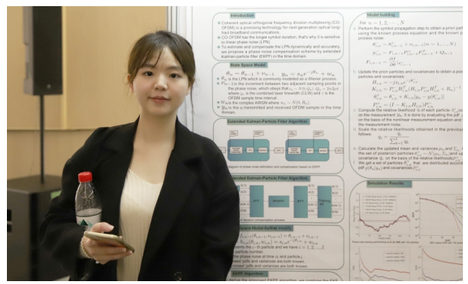

摘要：相干光正交频分复用(CO-OFDM)结合了正交频分复用、相干检测和光通信技术的优点，成为下一代光长距离宽带通信的有前途的技术。它具有频谱效率高、接收灵敏度高、色散容限高等优点。然而，与单载波系统相比，CO-OFDM 具有更长的符号持续时间，这就是为什么相干光正交频分复用 (CO-OFDM) 系统对线性相位噪声 (LPN) 比单载波系统更敏感的原因系统。本文提出了基于扩展卡尔曼粒子滤波器（EKPF）的实时动态补偿LPN。利用导频OFDM符号使相位噪声估计性能收敛到稳态，然后应用决策反馈算法进行进一步的估计和检测。通过与 16-QAM 100 Gbps CO-OFDM 系统中的传统贝叶斯滤波器进行动态跟踪误差和 BER 性能比较来进行仿真。仿真结果表明，与传统的贝叶斯滤波器相比，所提出的算法可以实现更准确的相位估计和误码率性能。因此，EKPF 结合了 EKF 和 PF 的优点，只需少量粒子即可提供时域相位噪声的准确估计。

statistics

Extended Kalman-Particle Filter-based Phase Noise Compensation for CO-OFDM Systems

北京师范大学 香港浸会大学 联合国际学院
BEIJING NORMAL UNIVERSITY · HONG KONG BAPTIST UNIVERSITY
UNITED INTERNATIONAL COLLEGE

Huiyun Deng[a] and Xinwei Du[a]
[a]Division of Science and Technology, BNU–HKBU United International College, Zhuhai, China

Introduction

- Coherent optical orthogonal frequency division multiplexing (CO-OFDM) is a promising technology for next-generation optical long-haul broadband communications.
- CO-OFDM has the longer symbol duration, that's why it is sensitive to linear phase noise (LPN)
- To estimate and compensate the LPN dynamically and accurately, we propose a phase noise compensation scheme by extended Kalman-particle filter (EKPF) in the time domain.

State Space Model

$$\theta_n = \theta_{n-1} + \nu_{n-1} \qquad y_n = s_n e^{-j\theta_n} + w_n$$

- θ_n is the LPN which is commonly modelled as a Wiener process.
- ν_{n-1} is the increment between two adjacent sampling points in the phase noise, which obeys that $\nu_n \sim N(0, Q_n)$, $Q_n = 2\pi\Delta\nu t$ where $\Delta\nu$ is the combined laser linewidth (CLW) and t is the OFDM sample time interval.
- w_n is the complex AWGN where $w_n \sim N(0, R_n)$.
- y_n is the n transmitted and received OFDM sample in the time domain.

Extended Kalman-Particle Filter Algorithm

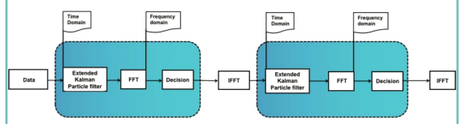

Block diagram of phase noise estimation and compensation based on EKPF.

Extended Kalman-Particle Filter Algorithm

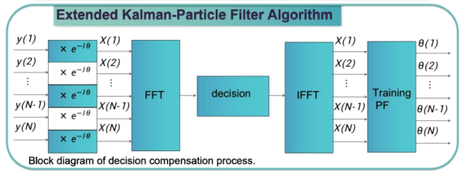

Block diagram of decision compensation process.

State Space Model-further modify

$$\theta_{i,n} = f_{i,n-1}(\theta_{i,n-1}, \nu_{i,n-1}) = \theta_{i,n-1} + \nu_{i,n-1}$$
$$y_{i,n} = h_{i,n}(\theta_{i,n}, w_{i,n}) = s_{i,n} e^{-j\theta_{i,n}} + w_{i,n}$$

- i represents the i- th particle and we have $i = 1, 2, ..., I$.
- I is the particle number.
- $\theta_{i,n}$ is the phase noise at time n and particle i .
- $w_{i,n}$ noises' pdfs and variances are both known.
- $\nu_{i,n-1}$ noises' pdfs and variances are both known.

EKPF Algorithm

- To derive the proposed EKPF algorithm, we combine the EKF and PF together.

Algorithm 1 EKPF Algorithm

```
function EKPF(True_phase, Observalue, Phase_initial)
    for each i ∈ [1, I] do
        Generate the particles θ^+_{i,0}(i = 1, ..., I) with only a loop (to store)
    end for
    for A doll n such that n ∈ [2, N]
        Sample from prior p(θ_n|y_n)
        Calculate the value of the sampled particles y_{i,n}
        Start EKF process and Generate Kalman filter gain K_{i,n}
        Calculate the weight of each particle; θ^+_n after EKF
        Normalized to get q_i
        for each i ∈ [1, I] do
            resample particles θ_{i,n}
        end for
    end for
end function
```

Model building

For $n = 1, 2, \cdots, N$

a. Perform the symbol propagation step to obtain a priori particles $\theta^-_{i,n}$, using the known process equation and the known pdf of the process noise:

$$\theta^-_{i,n} = \theta^+_{i,n-1} + \nu_{i,n-1}(n = 1, ..., N)$$
$$p^-_{i,n} = F_{i,n-1} P^+_{i,n-1} F^T_{i,n-1} + Q_{n-1}$$
$$F_{i,n-1} = \frac{\partial f}{\partial \theta}|_{\theta^+_{i,n-1}}$$

b. Update the priori particles and covariances to obtain a posteriori $\theta^-_{i,n}$ particles and covariances:

$$H_{i,n} = -j s_{i,n} e^{-j\theta^-_{i,n}}$$
$$K_{i,n} = P^-_{i,n} H^T_{i,n} (H_{i,n} P^-_{i,n} H^T_{i,n} + R_n)^{-1}$$
$$\theta^+_{i,n} = \theta^-_{i,n} + K_{i,n}[y_n - y(\theta^-_{i,n})]$$
$$P^+_{i,n} = (I - K_{i,n} H_{i,n}) P^-_{i,n}$$

c. Compute the relative likelihood q_i of each particle $\theta^+_{i,n}$ conditioned on the measurement y_n. It is done by evaluating the pdf $p(y_n|\theta^+_{i,n})$ on the basis of the nonlinear measurement equation and the pdf of the measurement noise.

d. Scale the relative likelihoods obtained in the previous step as follows: $q_i = \frac{q_i}{\sum_{k=1}^{I} q_k}$

e. Calculate the updated mean and variances μ_n and Σ_n. Generate the set of posteriori particles $\theta^+_{i,n} \sim \mathcal{N}(\mu_n, \Sigma_n)$ and update the covariance q_i on the basis of the relative likelihoods $P^+_{i,n}$.

f. We get a set of particles $\theta^+_{i,n}$ that are distributed according to the pdf $p(\theta_n|y_n)$ and covariances $P^+_{i,n}$.

Simulation Results

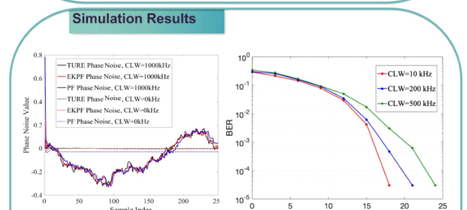

Phase noise tracking performance at 25 dB SNR with 100 particles.

BER versus SNR with 100 particles.

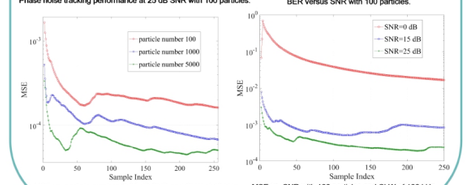

MSE vs. particle number at 25 dB SNR and CLW of 10 kHz. MSE vs. SNR with 100 particles and CLW of 100 kHz

Conclusion

- This research proposes an EKPF-based phase noise tracking algorithm for CO-OFDM systems.
- This approach combines the advantages of EKF and PF, which can provide an accurate estimate of time-domain phase noise with only a small number of particles.
- The use of PF improves the accuracy of EKF and EKF improves the stability of PF, so the combination of the two approaches can achieve better estimation performance of the phase noise.
- Simulation results verify the superior performance of the proposed EKPF algorithm with respect to accuracy and efficiency, compared with the conventional SIR particle filter.

Acknowledgements

- This graduation thesis was completed under the careful guidance of my advisor Xinwei Du. From the selection of the topic to the successful completion, Dr.Du gave me patient guidance and careful care. With the guidance of Dr.Du, I did not lose my way in the process of completing my graduation thesis, nor did I feel lost and helpless when modifying the program again and again. Dr.Du has a rigorous scientific attitude, agile thinking mode, patient teaching spirit and a working style of excellence. These are the abilities and qualities that I admire. Thanks to Dr.Du for giving me this learning opportunity.

The Organizing Committee of the 10th Science & Technology Poster Presentation
第十届理工科技学部海报展筹备委员会

Chairman: Dr. Alan Wai-Lun LAI (Programme Director of Applied Psychology)
主席：黎伟麟博士（应用心理学专业课程主任）

Secretary: Ms. Sherry Yuemei MO
秘书：莫月媚女士

Members of Organizing Committee: (Alphabetic order by Last Name without particular order)
筹备委员会成员：（以姓氏字母排序，排序不分先后）

- Dr. A.M. Elsawah (Statistics)
  A.M. Elsawah博士（统计学专业）
- Dr. Jefferson Fong (Computer Science and Technology)
  方子风博士（计算机科学与技术专业）
- Dr. Rui Meng (Data Science)
  孟蕊博士（数据科学专业）
- Dr. Xucheng Meng (Applied Mathematics)
  蒙许成博士（应用数学专业）
- Dr. Ya Wang (Food Science and Technology)
  王娅博士（食品科学与工程专业）
- Dr. Zijian Wang (Environmental Science)
  王子键博士（环境科学专业）
- Dr. Tianhao Zhi (Financial Mathematics)
  智天皓博士（金融数学专业）

Administrative and logistic support: Ms. Grace Huimin CHEN, Mr. Jack Eryuan XIAO,
Ms. Alice Lisi FENG, Ms. Mary Qunying LIN, Ms. Yang LI
行政及后勤支援：陈慧敏女士、肖二元先生、冯丽斯女士、林群英女士、李杨女士

Acknowledgements:
The organizing committee would like to acknowledge and appreciate the financial support from BNU-HKBU United International College Division of Science and Technology (DST), great efforts given by all the judges and generous help from all participating Alumni and other involved staff members of DST, ECDO, ITSC, MPRO and AO.

论坛筹备委员会在此特别感谢北京师范大学-香港浸会大学联合国际学院理工科技学部（DST）的资金支持，各位裁判员的辛苦付出，以及参与活动的所有校友与DST、ECDO、ITSC、MPRO和AO的相关工作人员所提供的无私帮助。

Published by
BNU-HKBU United International College
22 April, 2022

The Judging Pannel of the 10th Science & Technology Poster Presentation
第十届理工科技学部海报展裁判委员会

Head Judge: Prof. Jianhui LI, Prof. Weiwei SUN, Prof. Qingguo WANG
首席裁判：李建会教授，孙伟伟教授，王庆国教授

Chief Consultant: Prof. Weiwei SUN
总策划：孙伟伟教授

Invited External Judges: (Alphabetic order by Last Name without particular order)
受邀校外裁判：（以姓氏字母排序，排序不分先后）

- Dr. Lei Pang (ZUGO Intelligent Technology Co., Ltd, CTO)
  庞磊博士（珠高智能科技有限公司，首席技术官）
- Dr. Kai Wang (Associate professor of Cognitive neuroscience, South China Normal University)
  王凯副教授（华南师范大学认知神经科学副教授）
- Prof. Mingfu Wang (Institute for Advanced Study, Shenzhen University)
  王明福教授（深圳大学高等研究院教授）
- Prof. Lihua Yang (Associate Professor at Marine Science Department of SYSU)
  杨丽华教授（中山大学海洋科学学院副教授）
- Dr. Libin Zheng (Associate Professor of School of Artificial Intelligence, Sun YAT-SEN University)
  郑立彬副教授（中山大学人工智能学院副教授）
- Ms. Xueying Zou (Zhuhai Institute of Advanced Technology Chinese Academy of Sciences, Investment Analyst)
  邹雪莹女士（珠海中科先进技术研究院投资专员）

Internal Judges: (Alphabetic order by Last Name without particular order)
校内裁判：（以姓氏字母排序，排序不分先后）

- Dr. Xiaofeng Cai (Assistant Professor of Applied Mathematics Programme, UIC)
  蔡晓峰博士（理工科技学部应用数学专业助理教授）
- Dr. Meng He (DBM, Assistant professor of Accounting)
  何朦博士（工商管理学院会计学专业助理教授）
- Mr. LAM Mo, Brian (Lecturer, Accounting program, Division of Business Management)
  林武先生（工商管理学院会计学专业讲师）
- Mr. Tian Tang (Lecturer of Data Science Programme, UIC)
  唐天先生（理工科技学部数据科学与大数据技术专业讲师）
- Dr. May Wang (DBM, Associate Professor, PD of MMGT)
  王莹博士（工商管理学部副教授、传媒管理专修课程主任）
- Dr. Chiu Fai Wong (Assistant Professor of Financial Mathematics Programme, UIC)
  王朝辉博士（理工科技学部金融数学专业助理教授）
- Dr. Eason Xun Li (Assistant Professor of Environmental Science Programme, UIC)
  李迅博士（理工科技学部环境科学专业助理教授）
- Dr. Pengfei Zhao (Assistant Professor of Financial Mathematics Programme, UIC)
  赵鹏飞博士（理工科技学部金融数学专业助理教授）